

Biophysical Journal, Volume 98

Supporting Material

Alzheimer's A β (1-40) amyloid fibrils feature size dependent mechanical properties

Zhiping Xu, Raffaella Paparcone, and Markus J. Buehler

Supporting Information

SUPPORTING METHODS

1. Elastic Network Model

To simulate the mechanical properties of amyloid fibrils based on atomistic level structure information, here we use the elastic network model (ENM), originally proposed by Tirion (37) and later extended by Hinsen and colleagues (38, 39)). In the elastic network model, all atoms are represented by sites connected through linear Hookean springs with energy $E = k(r - r_0)^2$, with a cutoff distance R_c . The spring has length of its initial value as the reference distance r_0 . The hierarchy of interatomic interactions is described by either a constant k in Tirion's original version (37) or by a function $k(r_{ij})$ decaying with distance r_{ij} , which is tunable by constant r_0 , as proposed in Hinsen's extension of the method, and used in our work (38, 39). We apply elastic network model formulation in which all atoms excluding hydrogen atoms are taken into account. The spring constants between atoms represent interatomic interaction strengths and are weighted by their initial distance:

$$k(r_{ij}) = k_0 \exp\left(\frac{r_0}{r_{ij}} - 1\right)^2 \quad (1)$$

where $k_0 = 100 \text{ kcal}/(\text{mol} \cdot \text{\AA}^2)$, r_{ij} is the distance between atoms in pair and $r_0 = 5 \text{ \AA}$ is a distance-weight parameter as defined in (38). In addition, the interactions between atoms are smoothly cut off in the range of 10 \AA (37). As shown in previous studies (31-34), the lower-frequency normal modes calculated from the elastic network model describe experimental measurements or standard empirical force field simulations with good agreement. These modes are collective and correspond to large amplitude movements and conformational changes of proteins, which are critical in defining their physiological functions, mechanical and thermodynamical properties.

2. Normal Mode Analysis

The ENM is widely used in normal mode analysis of large protein molecules, due to the linear elastic and pairwise nature of springs connecting atoms and the resulting computational efficiency. It is noted that if full atomistic, conventional force field methods were used the resulting normal mode analysis would quickly become computationally intractable. In our case only very short amyloid fibrils with a few layers would be accessible to the computational

approach, preventing us from understanding size effects of mechanical parameters at scales up to tens of nanometers.

The normal modes of a molecular assembly are calculated through diagonalizing the second derivative of the potential energy (or Hessian matrix):

$$H_{ij} = \frac{\partial^2 E}{\partial x_i \partial x_j}, \quad (2)$$

where E is the total potential energy of system, and x_i, x_j are perturbation of atomic position on atom i and j . The eigenvalues of mass-weighted Hessian matrix $H\phi = M^{-1/2}HM^{-1/2}$ give the frequencies of corresponding modes, where M is a diagonal matrix of atomic masses. The corresponding eigenvectors of $H\phi$ represent the mode shapes.

For macromolecules such as $A\beta(1-40)$ amyloid fibrils, the first six modes are the rigid body modes with zero frequencies (including: three translation and three rotation modes). Most of the next higher modes (modes are ranked by eigenvalues from low to high) with low frequencies are collective modes, typically corresponding to elastic deformations such as twisting, bending and stretching (31-34). In the elastic network model, the Hessian matrices are often very sparse after introducing a cutoff range for the interaction. Thus diagonalizing these matrices requires much less computational effort and memory storage in comparison with full atomistic force field models. Although being very simple, the validity of the elastic network model as shown in eq. (1) for low frequency modes provides an accurate representation of the small-deformation (linear elastic) mechanical behavior of $A\beta(1-40)$ amyloid fibrils, as characterized by the collective modes with low frequencies (see also earlier studies using a similar approach (31-34)).

3. Extraction of Elastic Properties

Although the atomistic structure of the $A\beta(1-40)$ protein fibril suggests a high level of anisotropy due to the fact that interstrand hydrogen bonds have much lower stiffness than typical covalent bonds (≈ 2.10 kcal/mol/ \AA^2 for H-bonds (45), and ≈ 300 kcal/mol/ \AA^2 for covalent bonds (46) found in the backbone of protofibrils), Euler-Bernoulli beam models are widely used to identify a set of uncorrelated parameters, including: torsional modulus, bending rigidity and Young's modulus, in both experimental and simulation studies (22, 28, 30). In these approaches, critical issues including the anisotropy of the structure, the size-dependence of the mechanical

parameters with respect to the fibril length L and the coupling between different deformation modes are neglected.

For example, experimental approaches used to examine the mechanical properties of amyloid fibers of micrometer lengths are based on measuring thermal fluctuations (28) or on applying atomic force spectroscopy based bending (30). Subsequently, one-dimensional rod models with an invariant cross section are used in these analyses to extract the bending rigidity. However, as evidence from both experiment and atomistic simulations indicates, amyloid fibrils display a helical symmetry with a uniform twist along fiber axis (47). The full helical pitch of amyloid fibril has been evaluated in the range of ≈ 130 nm for 2-fold symmetric fibrils, and ≈ 82 nm for 3-fold symmetric fibrils (10, 36), that is, consistently on the order of ≈ 100 nm. When the amyloid fibril length is below or around this length scale, a significant change of the cross-sectional shape and orientation occurs along the fibril axis (10). This change will break the symmetry associated with the use of an isotropic rod model and is expected to introduce a strong fibril length-dependence of its mechanical properties, a feature not captured in classical rod models. Moreover, since amyloid fibrils are layered helical structures, their bending deformation may be coupled with interstrand shear or torsion, which may also result in the failure of the rod model.

In contrast to applying force or strain loads, the normal mode decomposition of macromolecular motions provides a specific frequency and stiffness for each mode, bypassing the above mentioned issues and thus offers direct information on the elastic constants of an equivalent continuum model of the amyloid fibril. Provided that the collective motion of the amyloid fibrils corresponds directly (or closely) to the deformation modes assumed in a continuum model, the parameters extracted from a normal mode analysis could be related to the elastic constants in continuum models (s.a. Young's modulus).

In continuum dynamics, the vibration of structures can be described by the equations of motion with strain field variables. For the torsional motion with respect to the fibril axis, the torsion field $\varphi = \varphi(z, t)$ represents the twist per unit length along the fibril axis, at position z and time t . For a linear rod, the resistance to torsional loading along the axis can be quantified as torsional or shear modulus G . The equation of motion is then written as

$$r I \frac{\partial^2 j}{\partial t^2} = G I \frac{\partial^2 j}{\partial z^2} \quad (3)$$

where ρ is the material density and I is the moment of inertia. For free vibrations without loading or displacement constraints, one can use $\left. \frac{\partial j}{\partial z} \right|_{z=0} = \left. \frac{\partial j}{\partial z} \right|_{z=L} = 0$ as the free ends boundary conditions, and solve the equation by introducing a solution of the form $j = j_0 \exp(i(kz - \omega t))$. The angular frequency ω for n -th order torsional mode can then be obtained as

$$\omega = k \sqrt{\frac{G}{r}}, \quad k = \frac{n\pi}{L}, \quad (4)$$

where L is fibril length and $n = 1, 2, 3$ is an integer representing the mode orders.

Similarly, the vibrational equation for transverse bending motion of the Euler-Bernoulli beam model can be written in

$$r A \frac{\partial^2 u}{\partial t^2} = - Y I \frac{\partial^2 u}{\partial z^2}, \quad (5)$$

where $D = YI$ is the bending rigidity, and $u = u(z, t)$ is the transverse displacement field as a function of the position z along the fibril axis and time t . Using $\left. \frac{\partial^2 u}{\partial z^2} \right|_{z=0} = \left. \frac{\partial^2 u}{\partial z^2} \right|_{z=L} = 0$ and

$\left. \frac{\partial^3 u}{\partial z^3} \right|_{z=0} = \left. \frac{\partial^3 u}{\partial z^3} \right|_{z=L} = 0$ as the free ends boundary conditions, the frequency for n -th order bending mode is given by

$$\omega = k^2 \sqrt{\frac{YI}{r A}}, \quad k = \frac{C_n}{L} \quad (6)$$

where C_n are numerical factors obtained by solving the eigenvalue problem (35) ($C_1 = 4.73$, $C_2 = 7.853$, $C_3 = 10.996$, $C_4 = 14.137$, $C_5 = 17.279 \dots$). It should be noted that the expression given in eq. (6) does not take into account any rotational and shear contribution, which may be important when a fiber features a low aspect ratio. To include this effect, more sophisticated models such as Timoshenko beam theory should be used (35).

For the axial stretching and compression modes, the longitudinal equation of motion is given by

$$r A \frac{\partial^2 u_z}{\partial t^2} = YA \frac{\partial^2 u_z}{\partial z^2}, \quad (7)$$

where u_z is the displacement along fibril axis direction. Again, by using the free ends boundary

conditions $\left. \frac{\partial u_z}{\partial z} \right|_{z=0} = \left. \frac{\partial u_z}{\partial z} \right|_{z=L} = 0$, the solution for n -th order stretching mode is

$$w = k \sqrt{\frac{Y}{r}}, \quad k = \frac{n\pi}{L} \quad (8)$$

where $c = \sqrt{Y/r}$ is the group speed for longitudinal waves (sound speed) of the linear elastic rod.

As discussed above, from the elastic network model we evaluate the frequencies and mode shapes by diagonalizing the Hessian matrix H' . We find that most (in short fibrils, we find modes that arise from localized deformation of the protofibril at the ends) of the lower frequency modes resemble the twisting, bending and stretching motion, corresponding to a continuum rod model. By equating the calculated frequencies with the expressions of the solutions of eqs. (4), (6) and (8), the key mechanical properties of $A\beta(1-40)$ amyloid fibril are obtained.

SUPPORTING MOVIES

Supporting Movies M1-M4: Animation GIF files show twisting (M1), bending (M2 and M3) as well as stretching (M4) modes of 2-fold symmetric amyloid fibril with $L = 19.28$ nm (40 layers).

Supporting Movies M5-S8: Animation GIF files show twisting (M5), bending (M6 and M7) as well as stretching (M8) modes of 3-fold symmetric amyloid fibril with $L = 19.4$ nm (40 layers).

SUPPORTING FIGURES

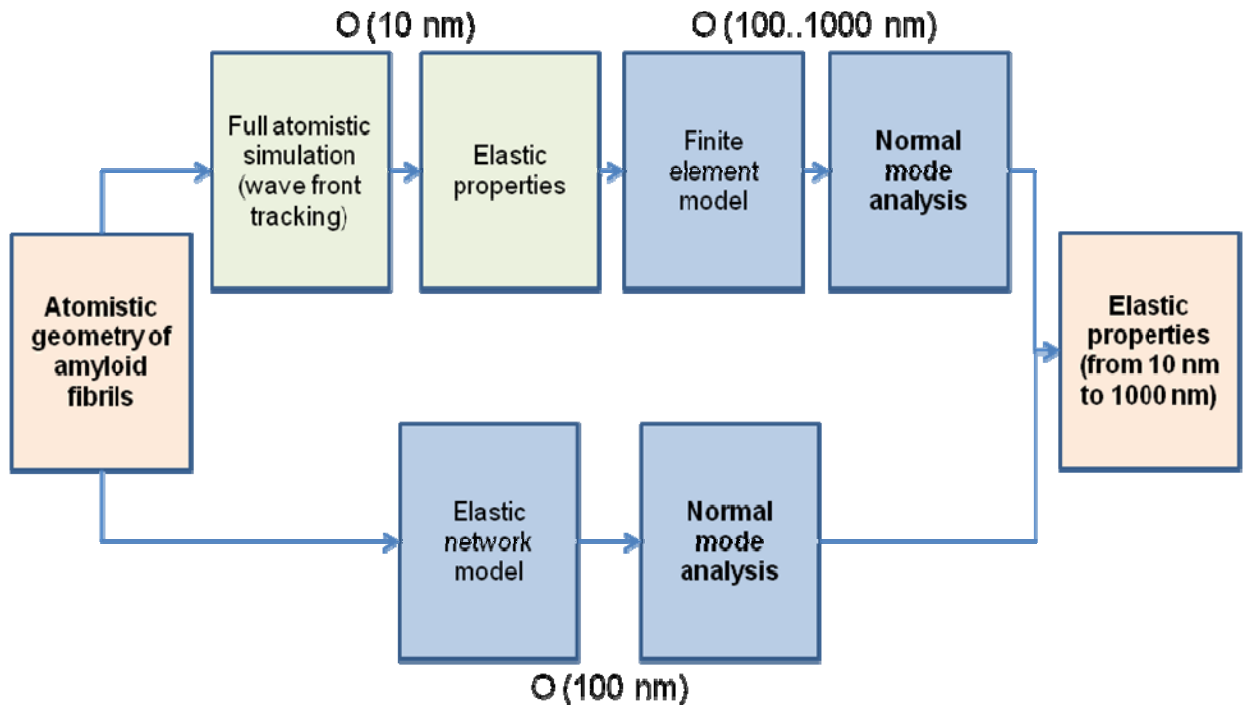


Figure S1: Overall approach used in this study, including relevant length-scales covered by each method. The atomistic geometry serves as the starting point for both the finite element based normal mode analysis and the elastic network model based normal mode analysis. For the finite element, we carry out full atomistic wave tracking simulations to extract the Young's modulus, which serves as an input parameter for the finite element model. In the case of the elastic network model, the atomistic geometry of amyloid fibrils is directly taken as the input.

Table S1: Normal modes shapes of $A\beta$ (1-40) amyloid fibrils (modes lower than the 7th mode correspond to rigid body motions, including three translation modes and three rotation modes); results from ENM simulations.

Structure	Length (in nm) (number of layers, N_{layers})	7 th	8 th	9 th	10 th	11 th	12 th	13 th	16 th	22 ^t _h
2-fold symmetric structure	9.64 (20)	T	B	B*	2 nd B	2 nd T	2 nd B*		S	
	19.28 (40)	B	T	B*	2 nd B	2 nd T	2 nd B*	S		
	28.92 (60)	B	B*	T	2 nd B	2 nd B	2 nd T	S		
3-fold symmetric structure	9.7 (20)	B	B	Br	Br	Br		2 nd T		S
	19.4 (40)	B	B	T	2 nd B	2 nd B	2 nd T	S		
	29.1 (60)	B	B	T	2 nd B	2 nd B	2 nd T	S		

N_{layers} : number of protofibril layers in the $A\beta$ (1-40) amyloid fibril. T: twisting (or torsional) mode, B: bending mode, B*: bending mode in the stiff direction in short 2-fold symmetric structures, S: stretching mode, Br: breathing mode. Modes not noted are those mixing several mode shapes.

Table S2: Frequencies of amyloid fibrils collective modes; results from ENM simulations.

Structure	Length (nm) (N_{layers})	Torsion (in THz)	Bending (in THz)	Bending (in THz)	Stretching (in THz)
2-fold symmetric structure	9.64 (20)	0.569	0.727	0.872	1.378
	14.46 (30)	0.389	0.405	0.481	0.925
	19.28 (40)	0.294	0.250	0.301	0.695
	24.1 (50)	0.236	0.169	0.204	0.557
	28.92 (60)	0.197	0.121	0.146	0.464
3-fold symmetric structure	9.7 (20)	-	0.555	0.610	1.020
	14.55 (30)	0.331	0.353	0.373	0.707
	19.4 (40)	0.252	0.229	0.242	0.534
	24.25 (50)	0.201	0.159	0.169	0.429
	29.1 (60)	0.168	0.117	0.123	0.358

Table S3: Key mechanical properties of $A\beta$ (1-40) amyloid fibrils with different lengths; results from ENM simulations.

Structure	Length (nm) (in N_{layers})	Torsional Modulus (in GPa)	Bending Rigidity (in 10^{-25}Nm^2)	Bending Rigidity (in 10^{-25}Nm^2)	Young's Modulus (in GPa)
2-fold symmetric structure	9.64 (20)	5.190	2.127	3.061	30.438
	14.46 (30)	5.458	3.342	4.715	30.859
	19.28 (40)	5.542	4.025	5.835	30.970
	24.1 (50)	5.580	4.491	6.543	31.082
	28.92 (60)	5.583	4.774	6.950	31.060
3-fold symmetric structure	9.7 (20)	-	1.758	2.124	17.641
	14.55 (30)	4.180	3.600	4.021	19.070
	19.4 (40)	4.307	4.790	5.349	19.341
	24.25 (50)	4.282	5.672	6.368	19.504
	29.1 (60)	4.307	6.329	6.995	19.559